A conceptual model for sheet-flow drawn from rapid granular flow theories.

Rui M. L. Ferreira[1], Vanessa A. Nicolau[2], Sílvia R. Amaral[3],
João G. A. B. Leal[4] & António B. Almeida[5]

[1] CEHIDRO-Instituto Superior Técnico, TULisbon, Av. Rovisco Pais, 1049-001 Lisboa, Portugal, ruif@civil.ist.utl.pt
[2] CEHIDRO-Instituto Superior Técnico, TULisbon, Av. Rovisco Pais, 1049-001 Lisboa, Portugal, vanessa.nicolau@gmail.com
[3] Laboratório Nacional de Engenharia Civil, Av. do Brasil, 101, 1700-066 Lisboa, Portugal, samaral@lnec.pt
[4] Dept. of Civil Engineering, Faculty of Sciences and Technology, UNL, Quinta da Torre, 2829-516 Caparica, Portugal; e-mail: jleal@fct.unl.pt
[5] CEHIDRO-Instituto Superior Técnico, TULisbon, Av. Rovisco Pais, 1049-001 Lisboa, Portugal, aba@civil.ist.utl.pt

ABSTRACT

This paper is aimed at presenting i) a simple, yet sound, conceptual model applicable to the simulation of erosion, deposition and transport of cohesionless sediment in stratified flows under high shear stresses and ii) numerical solutions in idealized unsteady flow non-equilibrium transport situations. The conceptual model for the granular phase comprises 2DV mass and momentum and energy equations and constitutive equations, all derived within the dense limit of the Chapman-Enskog kinetic theory. 1D shallow-flow conservation and closure equations are derived for the fluid-granular mixture. Formulas for the average velocity in the transport layers, the vertical net flux of sediment mass and the thickness of the transport layer are thus obtained. Numerical solutions for dam-break flows over cohesionless mobile beds in prismatic and non-prismatic channels are obtained and discussed.

Keywords: Granular flows, sheet-flow, dam-break

1 INTRODUCTION

This paper is consecrated to the development of a one-dimensional conceptual model applicable to flows with high geomorphic potential, herein geomorphic flows. A large number of flows can be included in this category, including rock or snow avalanches, debris flows or river flows in the upper regime exhibiting sheet flow. They have in common the ultimate driving mechanism, gravity, the fact that they are slender flows and the fact that they occur at or generate high shear stresses. Another common feature is the importance of the micromechanical characteristics of the sediment in the definition of the constitutive equations.

Given the common features, the conceptual model will be developed for sheet-flows, i.e. clearly stratified flows with a transport layer under high shear stresses, but is expected to be applicable also to debris-type flows, i.e. flows of a dense mixture of granular material and water whose transport layer occupies the full flow depth.

To ensure theoretical consistency and simplicity, both conservation and closure equations are deduced from the same theoretical body, the Chapman-Enskog theory for dense gases (Chapman & Cowling 1970, §16). Applications to granular flows have been accomplished by Lun et al. (1984), Jenkins & Richman (1988) or Armanini et al. (2005), among others. Should the flowing particles be considered

smooth, round and only slightly inelastic the kinetic theory requires only small modifications in order to provide 2DV conservation laws for the mass, momentum and fluctuating energy of the granular material and constitutive equations for the stress tensor, conductivity and viscosity coefficients and dissipation rate. The inclusion of frictional effects and viscous fluid-grain interactions is done by patching in *ad hoc* theories (Ferreira 2005, p. 249). The 2DV conceptual model is presented in Section 2. In the same section, the 2DV equations are depth-averaged, in accordance with the shallow-flow hypothesis and with appropriate kinematic boundary conditions. The continuum hypothesis is employed to merge the necessary conservation equations expressing 1D mass and momentum conservation.

In Section 3, the closure equations are obtained by process of numerical experimentation. The 2DV conservation and constitutive equations of the transport layer are solved in steady uniform conditions. Formulae for the average velocity in the transport layers, the vertical net flux of sediment mass and the thickness of the transport layer are obtained.

As they generate both sheet-flows and debris-like flows, dam-break flows are adequate to test the solutions of the conceptual model. Numerical solutions obtained for dam-break flows over cohesionless mobile beds, in prismatic and non-prismatic channels, are presented in Section 4.

2 CONSERVATION EQUATIONS

Sheet-flow is a two-dimensional stratified flow involving a mixture of water and granular material, picked up from the bottom. The granular phase is composed of cohesionless sediment grains, nearly elastic, slightly rough and approximately spherical. The fluid is viscous and incompressible. The flow structure is depicted in Figure 1. Three main layers are promptly identified: A, characterized by small mean sediment concentrations or by clear water and where turbulent stresses are dominant; B a transport layer, featuring decreasing concentrations upwards and stresses mainly originated in the granular phase and C the bed, composed of grains with no appreciable horizontal mean motion.
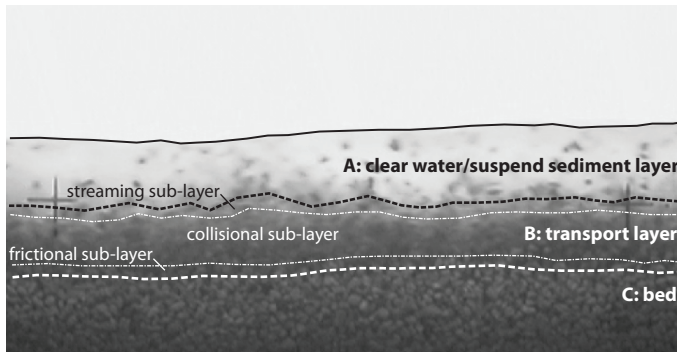

Figure 1. Detail of a sheet-flow with highlighted layered structure.

In layer B, it is expected that granular collisional stresses are dominant except in a thin bottom boundary layer where frictional stresses are dominant. The collisional dominance assumption simplifies the expressions of the bulk granular viscosity and of the granular conductivity (details in Ferreira 2005, pp. 231-250).

The 2DV conservation equations of layer A are the Reynolds-averaged Navier-Stokes equations. For layer B, the mass and momentum conservation equations, derived within the framework of the Chapman-Enskog theory, are, respectively

$$\rho^{(g)} D_t \left(\nu \right) + \rho^{(g)} \nu u_{i,i}^{(g)} = 0 \tag{1}$$

$$\rho^{(g)} \nu D_t \left(u_j^{(g)} \right) = -P_{,j}^{(g)} + T_{ij,i}^{(g)} + \rho^{(g)} \nu g_j + f_j^{(gw)} \tag{2}$$

$$\tfrac{3}{2}\rho^{(g)}\nu D_t\left(\Theta\right) = -\Phi_{i,i} + T_{ij}^{(g)}u_{j,i}^{(g)} - \gamma^{(gw)} \qquad (3)$$

where $\rho^{(g)}$ is the density of the sediment grains, nu is the solid fraction (concentration at a specific point in the flow), $u_i^{(g)}$ is the velocity field of the granular phase, $P^{(g)}$ is the granular pressure, $T_{ij}^{(g)}$ is the granular stress tensor, $f_j^{(gw)}$ is the force per unit volume expressing the interaction (essentially of viscous nature) of fluid and granular phases, Θ is the granular temperature, Φ_i is the flux of fluctuating energy and $\gamma^{(gw)}$ is the rate of dissipation, due to inelastic collisions and viscous damping (details in Ferreira 2005, pp. 247-249), of the fluctuating energy. In equations (1) to (3) the operator $D_t(\cdot)$ stands for the material derivative for which the convective operator is relative to the mean low, Einstein's notation is used for space derivatives and the bracket operator $\langle\cdot\rangle$ stands for point-wise time or ensemble average (ergodicity is assumed). Equation (3) reveals that, unlike thermodynamic systems a granular system can maintain a steady state of agitation, characterized by a given granular temperature, if and only if the rate of production equals the diffusive flux and the dissipation, i.e. if $T_{ij}^{(g)}u_{j,i}^{(g)} = \Phi_{i,i} + \gamma^{(gw)}$.

Conservation equations are also needed for the water phase. These can be obtained from a control volume analysis within the continuum hypotheses:

$$-\rho^{(w)}D_t\left(\nu\right) + (1-\nu)\,\rho^{(w)}u_{i,i}^{(w)} = 0 \qquad (4)$$

$$(1-\nu)\,\rho^{(w)}D_t\left(u_j^{(w)}\right) = -P_{,j}^{(w)} + T_{ji,i}^{(w)} + (1-\nu)\,\rho^{(w)}g_j - f_j^{(gw)} \qquad (5)$$

where $\rho^{(w)}$ is the density of the fluid, $u_{i,i}^{(w)}$ is the fluid velocity field, $P^{(w)}$ is the isotropic fluid pressure, $T_{ij}^{(w)}$ is the fluid stress tensor.

In order to derive the 1D conservation equations, i) the 2DV equations of conservation of each constituent are summed (equations 1 and 4 and 2 and 5), ii) cinematic boundary conditions are applied the free-surface, bed and margins and iii) the equations are depth-integrated, within the continuum hypothesis. The 1D conservation of total mass is

$$\partial_t A + \partial_x\left(uh\right) = -\partial_t A_0 = -\left(\frac{Q_b - Q_b^*}{(1-p_b)\Lambda} - A_l\right) \qquad (6)$$

where $A = A_w + A_b$, $A_b = \int_0^{h_b}\sigma(\eta)d\eta$ is the area of the cross-section occupied by layer B, h_b is the thickness of layer B, A_w is the area corresponding to layer A, A_0 is the area below the channel (the channel bed), $Q_b = C_b u_b A_b$ is the actual volumetric sediment discharge, C_b is the actual sediment concentration, $Q_b^* = C_b^* u_b A_b$ is the equilibrium sediment discharge, C_b^* is the equilibrium sediment concentration, u_b is the velocity of B, p_b is bed porosity, Λ is an adaptation length (the length scale of non-equilibrium sediment transport) and A_l is the lateral contribution of mass from the channel banks. In the proposed model, the calculation of A_l is simplified, as shown in Figure 2.
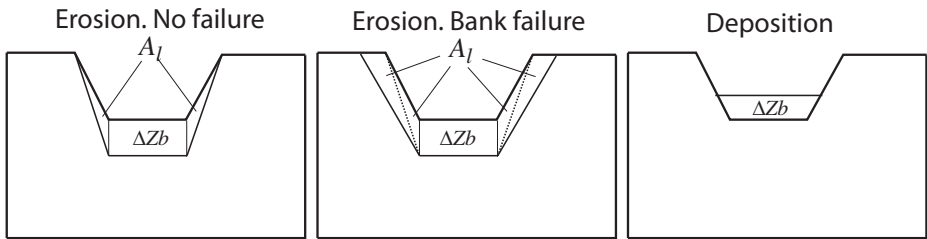

Figure 2. Idealization of lateral channel erosion.

The equation of conservation of total momentum is

$$\partial_t M + \partial_x \left(\rho_b u_b^2 A_b + \rho^{(w)} u_w^2 A_w + \rho_b g I_b + \rho^{(w)} g I_w\right)$$
$$+ g\left(\rho_b A_b + \rho^{(w)} A_w\right)\partial_x Z_b = -\tau_b P + g\rho_b K_b + g\rho^{(w)} K_w \quad (7)$$

where Z_b is the bed elevation, $M = \rho_b A u$ is the mass discharge, u is the layer-averaged velocity, u_w is the velocity of layer A, τ_b is the bed shear stress, P is the wetted perimeter, $\rho_b = \rho^{(w)}\left(1 + (s-1)C_b\right)$, $s = \rho^{(g)}/\rho^{(w)}$ and I_b, I_w, K_b and K_w are impulsion terms.

The equation of conservation of mass in the transport layer is

$$\partial_t H_b + \partial_x \left(H_b u_b\right) = -\left(\frac{Q_b - Q_b^*}{\Lambda} - T(1 - p_b)\right) \quad (8)$$

where the conservative variable is $H_b = A_b C_b$.

The equation of conservation of the bed is

$$(1 - p_b)\partial_t A_0 = \frac{Q_b - Q_b^*}{\Lambda} - A_l(1 - p_b) \quad (9)$$

The system of equations (6), (7), (8) and (9) admits four unknowns, the conservative variables A, M, H_b and A_0. At each time step, the primitive variables u, C_b must be computed from the conservative ones.

Closure equations for h_b, u_b, τ_b, C_b^* and Λ are needed. They will be derived in the next section within the same granular dynamics paradigm.

3 CLOSURE EQUATIONS

Numerical experiments are performed to derive the closure equations. A detailed characterization of the two-dimensional (vertical) flow in the transport layer is obtained by solving numerically the following set of ODEs

$$\frac{d\mathbf{Y}}{dz} = \mathbf{M}(\mathbf{Y}, z) \quad (10)$$

where $\mathbf{Y} = \begin{bmatrix} T^{(g)} & P^{(g)} & u_x^{(g)} & \Theta & \Phi & \nu & T^{(w)} & P^{(w)} & u_x^{(w)} \end{bmatrix}^{\mathrm{T}}$ and

$$\mathbf{M}(\mathbf{Y}, z) = \begin{bmatrix} -\rho^{(g)}\nu g \sin(\beta) - f_D \\ -\rho^{(w)}(s-1)\nu g \\ \frac{5\pi^{1/2}}{8}\frac{T^{(g)}}{\nu\rho^{(g)}\vartheta_1\vartheta_3 d_s}\frac{1}{\Theta^{1/2}} \\ -\frac{\pi^{1/2}}{4}\frac{1}{\nu\rho^{(g)}\vartheta_1\vartheta_4}\frac{\Phi}{d_s\Theta^{1/2}} \\ \frac{5\pi^{1/2}}{8}\frac{\left(T^{(g)}\right)^2}{\nu\rho^{(g)}\vartheta_1\vartheta_3}\frac{1}{d\Theta^{1/2}} - \frac{24}{\pi^{1/2}}\left(1 - e^{(gw)}\right)\rho^{(g)}\nu\vartheta_1\frac{\Theta^{3/2}}{d} \\ \frac{\pi^{1/2}}{4}\frac{1+\vartheta_1}{\rho^{(g)}\vartheta_1\vartheta_4\left(1+8\vartheta_1+4\nu^2\frac{dg_0}{d\nu}\right)}\frac{\Phi}{d\Theta^{3/2}} - \frac{s-1}{s}\frac{g\nu}{\left(1+8\vartheta_1+4\nu^2\frac{dg_0}{d\nu}\right)\Theta} \\ -\rho^{(w)}(1-\nu) g \sin(\beta) + f_D \\ -\rho^{(w)} g \\ \left(\frac{T^{(w)}}{\rho^{(w)}}\right)^{1/2}\frac{1}{\kappa z(1-\nu)^{1/2}f(\nu)} \end{bmatrix} \quad (11)$$

where β is the inclination of the channel, ϑ_1, ϑ_2, ϑ_3, ϑ_4, g_0 and $f(\nu)$ are functions of the solid fraction (details in Ferreira 2005, p. 246), $e^{(gw)}$ is the immersed restitution coefficient (Ferreira 2005, p. 248), κ is the Von Kármán constant and z is the vertical co-ordinate. It should be noted that the granular normal stresses are isotropic, hence reduced to the granular pressure $P^{(g)}$ and the mixture behaves as an incompressible fluid. This is a direct consequence of the dense limit approximation (details in Jenkins & Richman 1988, Ferreira 2005, pp. 231-238). System (11) must be solved simultaneously, subjected to 9 boundary conditions
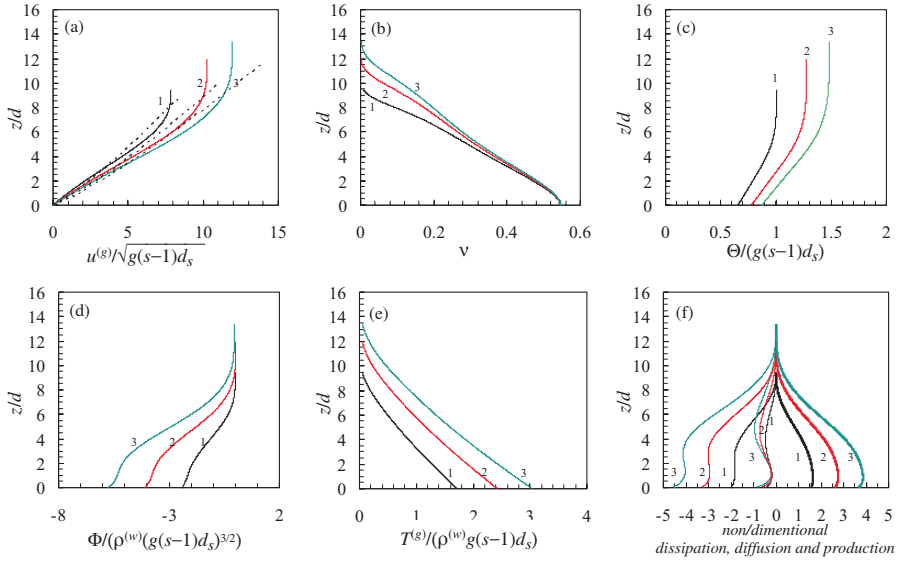
Figure 3. Computed profiles of non-dimensional quantities in the transport layer. Simulations 1, 2 and 3 correspond to, respectively, $\theta = 1.74, \theta = 2.49$ and $\theta = 3.07$.

(details in Ferreira 2005, pp. 252-256). The results for plastic pellets with $d = 0.003$ m, $s = 1.27$ and coefficient of restitution $e = 0.825$ are shown in Figure 3.

Equations for h_b, u_b, τ_b and $\phi_{s\,3,2}^{net} = (Q_b - Q_b^*)/\Lambda$ follow from the solution shown in Figure 3. The existence of a frictional layer across which the shear stress may vary allows for determining the mass flux between the bed and the transport layer. The integration of the equation of conservation of momentum in the vertical direction over the frictional layer renders (Ferreira (2005) p. 279)

$$\partial_t (A_0) = \phi_{3,2}^{net} = \frac{g\rho^{(w)}(s-1)\tan(\varphi_b)}{u_b (\rho_b u_x)|_{z=Z_f}} (Q_b - Q_b^*) \tag{12}$$

where Z_f is the elevation of boundary between the frictional and collisional layers. In equation (12) it is implicit that the equilibrium concentration is

$$C_b^* = C_f u^2 / (g(s-1)\tan(\varphi_b) h_b) \tag{13}$$

and the adaptation length is

$$\Lambda = \frac{u_b (\rho_b u_x)|_{z=Z_f}}{g\rho^{(w)}(s-1)(1-p_b)\tan(\varphi_b)} \tag{14}$$

As seen in Figures 3c and 3d, the the modulus of the flux of the fluctuating kinetic energy increases toward the bed and the granular temperature is never zero. This means that fluctuating energy is constantly being extracted from the mean flow and directed toward the bottom. As a consequence, the frictional sub-layer cannot increase indefinitely. It is assumed that this layer has a thickness of $2d$. The value of the concentration in ρ_b and of $(u_x)_{z=Z_f}$ can be read in Figures 3b and 3a, respectively. An estimate for the velocity in the transport layer can be obtained by fitting the profiles of Figure 3a:

$$u(z)/u = \tfrac{11}{6}(z/h)^{5/6} \tag{15}$$

where h is the flow depth. The depth-averaged velocity becomes

$$u_b/u = (h_b/h)^{5/6} \tag{16}$$

Depth-averaging the equation of conservation of the fluctuating energy, Ferreira (2005), pp. 278-287, obtained and algebraic relation for the thickness of the transport layer. Taking in account the values of the restitution coefficient and the internal friction angle at the bed, the non-dimensional thickness of the transport load layer appears to depend little on the type of sediment and may be approximated by

$$h_b/d = 1.7 + 5.5\theta \qquad (17)$$

In rivers undergoing sheet-flow, flow resistance is only marginally influenced by the particular shape of the stream bed, as alluvial bed forms are absent. The micromechanical properties of the sediment and the interaction with the fluid, in particular the energy dissipation in binary collisions and the interstitial viscous dissipation, are the mechanisms to accommodate in the characterization of the flow resistance. The results of Sumer et al. (1996) allow for the computation of the friction factor. It was found that the bed shear stress can be adequately described by $\tau_b \equiv \rho^{(w)}C_f u^2$ provided that the friction coefficient is

$$C_f = 0.02(h/d)^{-1/2}(w_s/u_*)^{-1/2} \qquad (18)$$

For practical purposes, the ratio u_*/w_s, where w_s is the fall velocity is considered to be 2.

4   COMPUTATIONAL RESULTS

The important formative potential of dam-break flows implies that they transport an extremely high sediment load over long distances. They generally feature debris-like characteristics at the wave front and a stratified sheet-like flow behind it. The overall quality of the model is thus tested in dam-break flows performed in idealized conditions, namely, instantaneous rupture and cohesionless mobile bed. Mathematically, it is a Riemann problem, a particular Cauchy problem.

Written in vector notation, the first order, non-homogeneous, hyperbolic system of conservation laws (equations 6, 7 and 8) that describe geomorphic dam-break flows is

$$\partial_t \left(\mathbf{V} \left(\mathbf{U} \right) \right) + \partial_x \left(\mathbf{F} \left(\mathbf{U} \right) \right) = \mathbf{G} \left(\mathbf{U} \right) \qquad (19)$$

where $\mathbf{V} : \mathbb{R}\mathbf{x}\,]0, +\infty[\rightarrow \mathbb{R}^3$ is the vector of dependent conservative variables, $\mathbf{U} : \mathbb{R}^3 \rightarrow \mathbb{R}^3$ is the vector of primitive variables, $\mathbf{F} : \mathbb{R}^3 \rightarrow \mathbb{R}^3$ is the flux vector, $\mathbf{G} : \mathbb{R}^3 \rightarrow \mathbb{R}^3$ is the vector of the source terms and x and t are the space and time co-ordinates, respectively.

A validation test was performed by comparing the results of the model with laboratory results performed at UCL, Louvain-la-Neuve, Belgium (details in Benoit 2005 pp. 56-56 and Ferreira et al. 2006). The sediment particles were PVC pellets with $s = 1.56$ kg m^{-3} and equivalent diameter $d = 3.9$ mm. The dimensions of the particles exhibited little variability. The initial conditions, in terms of h_L, the upstream water depth, Z_{b_L}, the upstream bed elevation, h_R, the downstream water depth, Y_L the upstream elevation above the upstream bed level, $\alpha \equiv \frac{h_R + \left|min\left(0, Z_{b_L}\right)\right|}{h_L + max\left(0, Z_{b_L}\right)}$ and $\delta \equiv \frac{Z_{b_L}}{h_L + max\left(0, Z_{b_L}\right)}$, are shown in Table 1.

Table 1. Summary of the initial data for experimental tests.

Name	h_L (m)	Y_{b_L} (m)	h_R (m)	Y_L (m)	α (−)	δ (−)
35_00_00	0.35	0.00	0.00	0.35	0.000	0.000
35_10_00	0.25	0.10	0.00	0.35	0.000	0.286
35_10_10	0.25	0.10	0.10	0.35	0.286	0.286

Equation (19) was discretized with a first-order Godunov scheme with HLLC Riemann solvers. The comparison between experimental and computational results is shown in Figure 4 where a general good agreement for the flow depth is

found, especially for the flat bed case (test 35_00_00). Tests 35_10_00 and 35_10_10 show two different types of hydraulic jump that may occur in the $\alpha - \delta$ plane (Ferreira 2005, Ferreira et al. 2006). Due to the low downstream water depth in test 35_10_00, the jump is induced by the non-equilibrium transport and friction (Capart & Young 1998). The the jump observed in 35_10_10 is independent of the source terms in equation (19). A general poor agreement in the bed elevation is found in the vicinity of the gate, due to un-acountable geotechnical slope failure.
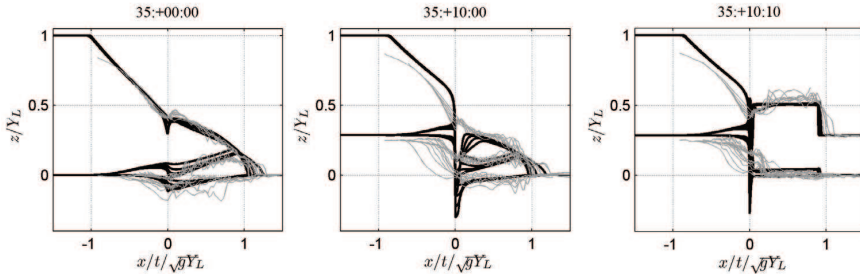

Figure 4. Computed and measured of the flow profiles corresponding to the tests identified in Table 1

In order to test the effects of the variability of channel configuration and the influence, on the final solution of the parameters that govern lateral bank failure, a test was performed with trapezoidal erodible banks. Initial conditions comprise: $Z_{b_L} = 0.06$ m, $h_L = 0.21$ m and $h_R = 0.0$ m. The initial bed width is $b_f = 0.15$ m and the inverse bank slopes are $m = 0.84$, which corresponds to an initial bank slope angle of 50°. This channel configuration mimics the experimental tests presented by Le Grelle et al. (2003). The material of the bed and margins is sand with $d = 1.8$ mm, $s = 2.62$, $\tan(\varphi_b) = 0.4$. For the sake of numerical stability, the friction coefficient was $C_f = 0.0067$.

Numerical results are obtained with a conservative firs order flux difference splitting discretization based on Euler's method and Roe's Riemann solvers (details in Ferreira 2005, pp. 465-479). The results are shown in Figure (5). Two scenarios are shown, SimBe1 for which the critical bank slope is $m_{cr} = 0.7$ and SimBe2 for which $m_{cr} = 0.825$. The equilibrium bank slope was, in both cases $m_{eq} = 0.839$.
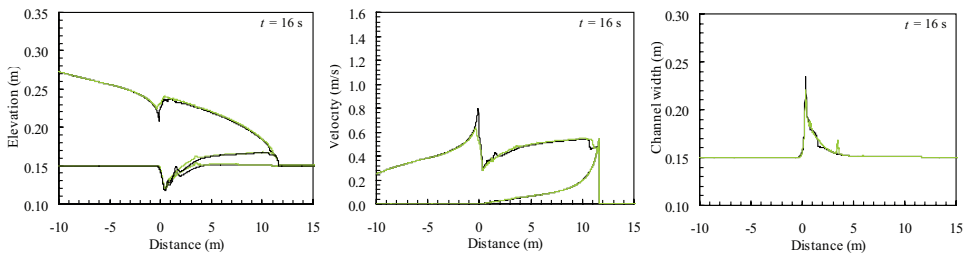

Figure 5. Longitudinal profiles of the flow depth, bed elevation and thickness of the transport layer (left), layer-averaged velocity and velocity in the transport layer (center) and channel width at the initial bed elevation (right). $X' = (x/t)/\sqrt{gY_L}$. Darker line: $m_c r = 0.7$. Lighter line: $m_c r = 0.825$

In scenario SimBe1 the critical value is attained infrequently but, when attained, the lateral sediment input is large and the local morphologic impact is significant. On the contrary, in SimBe2 the frequency of bank failure is high but

the corresponding volume of sediment is relatively mild. In both scenarios the total volume eroded from the banks is high and of the same order of magnitude; it is the rate at which it is eroded that is controlled by the value of m_{cr}. As a result, the impact of the particular choice of m_{cr} on the final solution is low. The main difference is that the flow profiles corresponding to scenario SimBe2 are smoother that those of SimBe1 because the flow was not subjected to massive bank avulsion events

5   CONCLUSION

The conceptual model presented in this paper is applicable to geomorphic stratified flows featuring sediment transport at high shear stresses. The dense limit of Chapman-Enskog's kinetic theory is at the root of the 1D closure equations. This means that the interaction between sediment and fluid phenomena is conceived to occur, fundamentally, at the grain-scale.

The model was tested for internal consistency and compared with experimental evidence. Dam-break flows were chosen as applications, for its ability to generate stratified flows with high shear stresses. The computational results suggest that the model assumptions, namely the emphasis on grain-scale phenomena as the most relevant for developing closure models, may be valid for a wider range of actual geomorphic flows.

ACKNOWLEDGMENTS

REFERENCES

Armanini, A.; Capart, H.; Fraccarollo, L.; Larcher M. (2005) Rheological stratification in experimental free-surface flows of granular-liquid mixtures. *J. Fluid Mech.* **532**:269-319 .

Capart, H. & Young, D.L. (1998) Formation of a jump by the dam-break wave over a granular bed. *J. Fluid Mech.* **372**:165-187.

Chapman, S. & Cowling, T. G. (1970). *The Mathematical Theory of Non-Uniform Gases,* 3rd Ed. Cambridge University Press.

Lun, K. K.; Savage, S. B.; Jeffery, D. J. & Chepurny, N. (1984) Kinetic theories for granular flows: inelastic particles in Couette flow and slightly inelastic particles in a general flow field. *J. Fluid Mech.* **140**: 223-256.

Ferreira, R. M. L., (2005) *River Morphodynamics and Sediment Transport. Conceptual Model and Solutions.* PhD Thesis, Instituto Superior Técnico, TU Lisbon.

Ferreira, R.M.L.; Amaral, S.; Leal, J.G.A.B. & Spinewine, B., (2006), Discontinuities in geomorphic dam-break flows. *River Flow 2006*, Vol. 1: 1521-1530, Balkema. ISBN0415408156.

le Grelle, N., Soares Frazão, S., Spinewine B. & Zech Y. (2003). Dam-break flow experiment: Geomorphic changes in a valley with uniform sediment. Proc. 3rd IMPACT Workshop, UCL Louvain-la-Neuve, 5-7 November.

Jenkins, J. T. & Richman, M. W. (1988) Plane simple shear of smooth inelastic circular disks: the anisotropy of the second moment in the dilute and dense limits. *J. Fluid Mech.* **192**:313-328.

Spinewine, B. (2005) *Two-layer flow behavior and the effects of granular dilatancy in dambreak induced sheet-flow.* PhD Thesis, Université catholique de Louvain, Louvain-la-Neuve.

Sumer, B. M.; Kozakiewicz, A.; Fredsøe, J. & Deigard, R. (1996) Velocity and Concentration Profiles in Sheet-Flow Layer of Movable Bed. *J. Hydraul. Eng.* **122**: 549-558.